Relativistic nuclear structure. I. Nuclear matter

R. Brockmann
Department of Physics, University of Mainz, D-6500 Mainz, Germany

R. Machleidt
Department of Physics, University of Idaho, Moscow, Idaho 83843
(Received 18 December 1989)

The formalism for the Dirac-Brueckner approach to the nuclear many-body problem is described including its basis in relativistic two-nucleon scattering. A family of relativistic meson-exchange potentials is constructed which (apart from the usual coupling terms for heavy mesons) apply the pseudovector (gradient) coupling for the interaction of pseudoscalar mesons (π,η) with nucleons. These potentials describe low-energy two-nucleon scattering and the deuteron data accurately. Using these potentials, the properties of nuclear matter are calculated in the Dirac-Brueckner-Hartree-Fock approximation, in which the empirical nuclear matter saturation is explained quantitatively. The effective two-body interaction in the nuclear matter medium (G matrix) is calculated directly in the nuclear matter rest frame. Thus, cumbersome transformations between the two-nucleon center-of-mass frame and the nuclear matter rest frame are avoided. Size and nature of relativistic effects included in the present approach are examined in detail. The formalism, the potentials, and the results of this paper may also serve as a basis and a realistic starting point for systematic relativistic nuclear structure studies as well as for the investigation of further relativistic many-body corrections and of contributions of higher order.

I. INTRODUCTION

One of the most fundamental challenges pervading theoretical nuclear physics for half a century is to understand the properties of nuclei in terms of the underlying interactions between the constituents. Historically, the first attempt was made by Heisenberg's student Euler who calculated the properties of nuclear matter in second-order perturbation theory[1] assuming nucleons interacting via a two-body potential of Gaussian shape. When the singular nature of the nuclear potential at short distances ("hard core") was realized, it became apparent that conventional perturbation theory is inadequate. Special many-body methods had to be worked out. Brueckner, Levinson, and Mahmoud[2] initiated a method which was further developed by Bethe[3] and Goldstone.[4] Alternatively, Jastrow[5] suggested to take a variational approach to the nuclear many-body problem.

In the 1960s substantial advances in the physical understanding of Brueckner theory were made due to the work by Bethe and co-workers (see, e.g., the review by Day[6]). Systematic calculations of the properties of nuclear matter applying Brueckner theory started in the late 1960s and continued through the 1970s (Refs. 7–9) (see Ref. 10 for a more recent summary).

The results obtained using a variety of nucleon-nucleon (NN) potentials show a systematic behavior: The predictions for nuclear matter saturation are located along a band which does not meet the empirical area (see Fig. 1 and Table I). [Various semiempirical sources suggest nuclear matter saturation to occur at an energy per particle $\mathcal{E}/A=-16\pm1$ MeV and a density which is equivalent to a Fermi momentum of $k_F=1.35\pm0.05$ fm^{-1} (Refs. 8 and 9).] This phenomenon is denoted by the "Coester band[22]." The essential parameter of the Coester band is the strength of the nuclear tensor force as measured by the predicted D-state probability of the deuteron or as expressed in the wound integral in nuclear matter (see Table I).[10]

The Brueckner-Goldstone expansion is believed to be convergent in terms of the number of hole lines. Calculations by Day[12,23] and Day and Wiringa[17] have confirmed this for the case of some realistic potentials. However, three- and four-hole line diagrams contribute about 5–7 MeV to the binding energy per nucleon at saturation (cf. Table I) and, thus, are not negligible. In Fig. 1 open symbols represent results obtained in the two-hole line approximation; symbols with a cross denote results including the contributions from three- and four-hole lines. It is seen that taking into account up to four-hole lines leads, indeed, to an improved Coester band as compared to the two-hole line approximation; however, the improvement is insufficient to explain the empirical saturation point.[24] Results based on the variational approach are in fair agreement with Brueckner theory predictions[17] and, thus, also fail to quantitatively explain nuclear saturation.

Since the mid-1970s, there have been comprehensive efforts to check Brueckner theory;[25] we mention here, in particular, the work using hypernetted chain theory.[25,26] Based on this work, there are indications that the two-hole line approximation of Brueckner-Bethe theory may

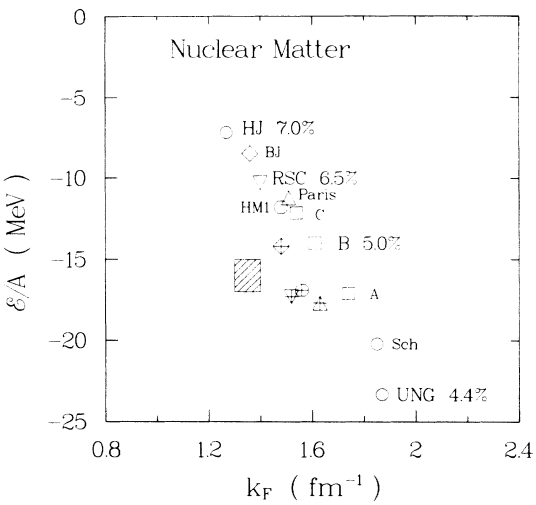

FIG. 1. Nuclear matter saturation as predicted by a variety of *NN* potentials (see Table I). Open symbols are saturation points obtained in the two-hole line approximation; symbols with a cross denote corresponding predictions with three- and four-hole lines included. Percent numbers refer to the *D*-state probability of the deuteron as predicted by the corresponding potential. The shaded area denotes the empirical value.

not necessarily be correct. Some published variational calculations are in fair agreement with Brueckner-Bethe results if three-hole lines plus a four-hole line estimate are included.[17]

Approaches discussed so far are based on the simplest model for the atomic nucleus: Nucleons obeying the nonrelativistic Schrödinger equation interact through a two-body potential that fits low-energy *NN* scattering data and the properties of the deuteron. The failure of this model to explain nuclear saturation indicates that we may have to extend the model. One possibility is to include degrees of freedom other than the nucleon. The meson theory of the nuclear force suggests to consider, particularly, meson and isobar degrees of freedom. Characteristically, these degrees of freedom lead to medium effects on the nuclear force when inserted into the many-body problem as well as many-nucleon force contributions (see Ref. 10 for a comprehensive review on this subject). In general, the medium effects are repulsive, whereas the many-nucleon force contributions are attractive. Thus there are large cancellations and the net result is very small. The density dependence of these effects/contributions is such that the saturation properties of nuclear matter are not improved.[10]

We note that the discussion of many-body force effects in the previous paragraph applies to approaches in which two- and many-body forces are treated on an equal footing; i.e., both categories of forces are based on the same meson-baryon interactions and are treated consistently (implying the quoted medium effects on the two-body force). The situation is different if the three-body force is introduced on an *ad hoc* basis with the purpose to fit the empirical nuclear matter saturation.[27] Such a three-body potential may be large, particularly, if the two-body force used substantially underbinds nuclear matter. By construction such a three-body force improves the equation of state of nuclear matter as well as the description of light nuclei.

Recently, also, quark degrees of freedom have been studied in nuclear matter.[28,29] However, the present calculations are not yet sufficiently sophisticated to be conclusive concerning the role of quarks in nuclear saturation.

In the 1970s a relativistic approach to nuclear structure was developed by Miller and Green.[30] They studied a Dirac-Hartree model for the ground state of nuclei which was able to reproduce the binding energies, the root-mean-square radii, and the single-particle levels, particularly the spin-orbit splittings. Their potential consisted of a strong (attractive) scalar and (repulsive) vector

TABLE I. Nuclear matter saturation properties as predicted by various *NN* potentials. Given are the saturation energy per nucleon, $\mathcal{E}/A$, and Fermi momentum k_F as obtained in the two-hole line approximation using the standard choice for the single-particle potential. Results including three- and four-hole line contributions are given in square brackets. The wound integral κ is given at $k_F = 1.35$ fm^{-1}. P_D is the predicted %-*D* state of the deuteron.

Potential	Reference[a]	P_D (%)	κ (%)	$\mathcal{E}/A$ (MeV)	k_F (fm^{-1})	Reference[b]
HJ	11	7.0	21	−7.2	1.27	12
BJ	13	6.6		−8.5[−14.2]	1.36[1.48]	12
RSC	14	6.5	14	−10.3[c][−17.3]	1.40[c][1.52]	15[12]
V_{14}	16	6.1	12[19]	−10.8[−17.8]	1.47[1.62]	17
Paris	18	5.8	11	−11.2[−17.7]	1.51[1.63]	18[17]
HM1	19	5.8	11	−11.8[−16.9]	1.48[1.56]	19[17]
Sch	20	4.9	8	−20.2	1.85	19
UNG	21	4.4	5	−23.3	1.87	19
(Bonn)*C*	10	5.6	8.1	−12.1	1.54	10
(Bonn)*B*	10	5.0	6.6	−14.0	1.61	10
(Bonn)*A*	10	4.4	5.4	−17.1	1.74	10

[a]References to the potentials.
[b]References for the nuclear matter calculations.
[c]Using OBEP for $J \geq 3$.

component. The Dirac-Hartree(-Fock) model was further developed by Brockmann,[31] Horowitz and Serot,[32] and Serot and Walecka.[33] At about that same time, Arnold, Clark, and Mercer applied a Dirac equation containing a scalar and vector field to proton-nucleus scattering.[34] The most significant result of this Dirac phenomenology is the quantitative fit of spin observables which are only poorly described by the Schrödinger equation.[35] This success and Walecka's theory on highly condensed matter[36] made relativistic approaches very popular.

Inspired by these achievements, a relativistic extension of Brueckner theory has been suggested by Shakin and co-workers,[37,38] frequently called the Dirac-Brueckner approach. The advantage of a Brueckner theory is that the free *NN* interaction is used; thus there are no parameters in the force which are adjusted in the many-body problem. The essential point of the Dirac-Brueckner approach is to use the Dirac equation for the single-particle motion in nuclear matter. In the work done by the Brooklyn group, the relativistic effect is calculated in first-order perturbation theory. This approximation is avoided, and a full self-consistency of the relativistic single-particle energies and wave functions is performed in the subsequent work by Brockmann and Machleidt[39,40] and by ter Haar and Malfliet.[41] Formal aspects involved in the derivation of the relativistic G matrix have been discussed in detail by Horowitz and Serot.[42,43]

The common feature of all Dirac-Brueckner results is that a (repulsive) relativistic many-body effect is obtained which is strongly density dependent such that the empirical nuclear matter saturation can be explained. In most calculations a one-boson-exchange (OBE) potential is used for the nuclear force. In Ref. 44 a more realistic approach to the *NN* interaction is taken, applying an explicit model for the 2π exchange that involves Δ isobars, thus avoiding the fictitious σ boson typically used in OBE models to provide intermediate-range attraction. It is found in Ref. 44 that the relativistic effect for the more realistic model is almost exactly the same as that obtained for OBE potentials. This finding seems to justify the use of the OBE model.

It is the purpose of this first paper in a series of papers to provide a basis and a realistic starting point for systematic relativistic nuclear structure calculations to be performed in the future. We will describe the Dirac-Brueckner formalism, and we shall construct a family of realistic and quantitative *NN* potentials which are appropriate for application to relativistic nuclear structure. Our presentation will be sufficiently detailed, such that the formalism is transparent and the results are reproducible for any researcher in the field. This first paper will be restricted to nuclear matter in the Dirac-Brueckner-Hartree-Fock approximation. The properties of finite nuclei will be studied in a forthcoming paper.[45] This paper may also serve as a basis for the consideration and calculation of further relativistic corrections and of contributions of higher order.

In Sec. II we present the formalism of the Dirac-Brueckner approach to nuclear matter. Section III contains results and a discussion. An outlook is given in Sec. IV. Many important mathematical details are given in the appendixes. In Appendix A the three-dimensional relativistic equation used in our work is derived. The relativistic OBE amplitudes defining the potential are given in Appendix B. Appendix C contains the parameters of the potentials and the predictions for the two-nucleon system. Finally, Appendix D contains quantitative results for nuclear matter in addition to those presented in Sec. III.

II. DIRAC-BRUECKNER APPROACH

As mentioned in the Introduction, the essential point of the Dirac-Brueckner approach is to use the Dirac equation for the single-particle motion in nuclear matter:

$$(\not{p}-M-U)\bar{u}(\mathbf{p},s)=0 \tag{1}$$

or, in Hamiltonian form,

$$(\boldsymbol{\alpha}\cdot\mathbf{p}+\beta M+\beta U)\bar{u}(\mathbf{p},s)=\epsilon_p\bar{u}(\mathbf{p},s)\ ,$$

with

$$U=U_S+\gamma^0U_V\ , \tag{2}$$

where U_S is an attractive scalar and U_V (the timelike component of) a repulsive vector field (notation as in Ref. 46; $\beta=\gamma^0$, $\alpha^l=\gamma^0\gamma^l$). M is the mass of the free nucleon.

The fields U_S and U_V are in the order of several hundred MeV and strongly density dependent (numbers will be given below). In nuclear matter they can be determined self-consistently. The resulting fields are in close agreement with those obtained in the Dirac phenomenology of scattering.

The solution of Eq. (1) is

$$\bar{u}(\mathbf{p},s)=\left[\frac{\tilde{E}_p+\tilde{M}}{2\tilde{M}}\right]^{1/2}\begin{bmatrix}1\\ \dfrac{\boldsymbol{\sigma}\cdot\mathbf{p}}{\tilde{E}_p+M}\end{bmatrix}\chi_s\ , \tag{3}$$

with

$$\tilde{M}=M+U_S\ , \tag{4}$$

$$\tilde{E}_p=(\tilde{M}^2+\mathbf{p}^2)^{1/2}\ , \tag{5}$$

and χ_s a Pauli spinor. The covariant normalization is $\bar{u}(\mathbf{p},s)\bar{u}(\mathbf{p},s)=1$. Note that the Dirac spinor [Eq. (3)] is obtained from the free Dirac spinor by replacing M by $\tilde{M}$.

As in conventional Brueckner theory, the basic quantity in the Dirac-Brueckner approach is a G matrix, which satisfies an integral equation. In this relativistic approach, a relativistic three-dimensional equation is chosen. Following the basic philosophy of traditional Brueckner theory, this equation is applied to nuclear matter in strict analogy to free scattering.

We choose the Thompson equation[47] [Eq. (A23) of Appendix A], which is a relativistic three-dimensional reduction of the Bethe-Salpeter equation.[48] Crucial for our choice is the fact that, in the framework of the Thompson equation, meson retardation is ignored (i.e., a static meson propagator is used). This is also true for the Blankenbecler-Sugar (BbS) equation,[49] Eq. (A18) of Appendix A. Note that in theories which incorporate

meson retardation, effects due to medium modifications on meson propagation in nuclear matter can be calculated. These effects have been investigated by the Bonn group (Ref. 10 contains a recent summary) and were found to be small and repulsive.[50] Thus these effects are known and are not very important, and for that reason we will ignore them (which a static theory will do). We mention that in some reductions of the Bethe-Salpeter equation, one nucleon is restricted to its mass shell.[20,51] This results in a wrong description of meson retardation. As a consequence, in this case the medium effect on meson propagation increases the binding energy substantially[52] (i.e., the medium effects on meson propagation come out wrong in sign and size). Thus another reason for ignoring meson retardation is to exclude any false medium effects on meson propagation from the outset. The variations in the results obtained from different equations, which, however, all use static meson propagators, are small (compare, e.g., the BbS and Thompson case in Fig. 16 of Ref. 43). To summarize, there exist many relativistic three-dimensional versions of the Bethe-Salpeter equation, which are all mathematically equally justified. However, some of these equations have unphysical features due to the approximations involved in their derivation. Now, when one discards these unphysical cases, then the ambiguities in the results due to different versions of the relativistic equation are rather small (much smaller than the relativistic effects we are going to calculate).

Including the necessary medium effects, the Thompson equation in the nuclear matter rest frame reads [cf. Eq. (A23) in Appendix A and subsequent discussion]

$$\tilde{G}(\mathbf{q}',\mathbf{q}|\mathbf{P},\tilde{z})=\tilde{V}(\mathbf{q}',\mathbf{q})+\int\frac{d^3k}{(2\pi)^3}\tilde{V}(\mathbf{q}',\mathbf{k})\times\frac{\tilde{M}^2}{\tilde{E}^2_{(1/2)\mathbf{P}+\mathbf{k}}}\frac{Q(\mathbf{k},\mathbf{P})}{\tilde{z}-2\tilde{E}_{(1/2)\mathbf{P}+\mathbf{k}}}\times\tilde{G}(\mathbf{k},\mathbf{q}|\mathbf{P},\tilde{z})\ , \tag{6}$$

with

$$\tilde{z}=2\tilde{E}_{(1/2)\mathbf{P}+\mathbf{q}}\ . \tag{7}$$

$\mathbf{P}$ is the c.m. momentum, and $\mathbf{q}$, $\mathbf{k}$, and $\mathbf{q}'$ are the initial, intermediate, and final relative momenta, respectively, of the two particles interacting in nuclear matter. The Pauli operator Q projects onto unoccupied states. In Eq. (6) we suppressed the k_F dependence as well as spin (helicity) and isospin indices. For $|\frac{1}{2}\mathbf{P}\pm\mathbf{q}|$ and $|\frac{1}{2}\mathbf{P}\pm\mathbf{k}|$, the angle average is used.

The energy per nucleon in nuclear matter, which is the objective of these calculations, is considered in the nuclear matter rest frame. Thus the G matrix is needed for the nuclear matter rest frame. Equation (6) gives this nuclear matter G matrix directly in that rest frame. Alternatively, one can calculate the G matrix first in the two-nucleon center-of-mass (c.m.) system (as customary in calculations of the $\mathcal{T}$ matrix in two-nucleon scattering) and then perform a Lorentz transformation to the rest frame. This method, which is described in detail in Ref. 43, is, however, complicated, involved, and cumbersome. The advantage of our procedure is that it avoids this complication. Further treatments of Eq. (6) can follow the lines established from conventional Brueckner theory, as, e.g., the use of the angle-averaged Pauli projector, etc. Numerically, the equation can be solved by standard methods of momentum-space Brueckner calculations.[7]

The essential difference to standard Brueckner theory is the use of the potential $\tilde{V}$ in Eq. (6). Indicated by the tilde, this meson-theoretic potential is evaluated by using the spinors of Eq. (3) instead of the free spinors applied in scattering as well as in conventional ("nonrelativistic") Brueckner theory (see Appendix B). Since U_S (and $\tilde{M}$) are strongly density dependent, so is the potential $\tilde{V}$. $\tilde{M}$ decreases with density. The essential effect in nuclear matter is a suppression of the (attractive) σ exchange; this suppression increases with density, providing additional saturation. It turns out (see figures below) that this effect is so strongly density dependent that the *empirical saturation and incompressibility* can be reproduced. Furthermore, the prediction for the Landau parameter f_0 is considerably improved without deteriorating the other parameters (see Table V below). Note that sum rules require $f_0>-1$ at nuclear matter density.[53]

The single-particle potential

$$U(m)=\frac{\tilde{M}}{\tilde{E}_m}\langle m|U|m\rangle=\frac{\tilde{M}}{\tilde{E}_m}\langle m|U_S+\gamma^0U_V|m\rangle=\frac{\tilde{M}}{\tilde{E}_m}U_S+U_V \tag{8}$$

is the self-energy of the nucleon, which is defined in terms of the G matrix formally in the usual way:

$$U(m)=\mathrm{Re}\sum_{n\le k_F}\frac{\tilde{M}^2}{\tilde{E}_n\tilde{E}_m}\langle mn|\tilde{G}(\tilde{z})|mn-nm\rangle\ , \tag{9}$$

where m denotes a state below or above the Fermi surface (continuous choice). The constants U_S and U_V are determined from Eqs. (8) and (9). Note that Eq. (2) is an approximation, since the scalar and vector fields are in general momentum dependent; however, it has been shown that this momentum dependence is very weak.[40]

Finally, the energy in nuclear matter is obtained in lowest order by

$$\frac{\mathcal{E}}{A}=\frac{1}{A}\sum_{m\le k_F}\frac{\tilde{M}}{\tilde{E}_m}\langle m|\boldsymbol{\gamma}\cdot\mathbf{p}_m+M|m\rangle+\frac{1}{2A}\sum_{m,n\le k_F}\frac{\tilde{M}^2}{\tilde{E}_m\tilde{E}_n}\langle mn|\tilde{G}(\tilde{z})|mn-nm\rangle-M\ . \tag{10}$$

In Eqs. (9) and (10) we use

$$\tilde{z}=\tilde{E}_m+\tilde{E}_n\ . \tag{11}$$

The expression for the energy [Eq. (10)] is denoted by the Dirac-Brueckner-Hartree-Fock (DBHF) approximation. If $\tilde{M}$ is replaced by M, we will speak of the Brueckner-Hartree-Fock (BHF) approximation, since this case, qual-

itatively and quantitatively, corresponds to conventional nonrelativistic Brueckner theory. Thus we will occasionally denote the DBHF calculation by "relativistic" and the BHF calculation by "nonrelativistic" (though, strictly speaking, all our calculations are relativistic).

In Eqs. (8)–(10) the states $|m\rangle$ and $|n\rangle$ are represented by Dirac spinors of the kind in Eq. (3) and an appropriate isospin wave function; $\langle m|$ and $\langle n|$ are the adjoint Dirac spinors $\bar{u}=u^{\dagger}\gamma^0$ with $\bar{u}u=1$; $\tilde{E}_m\equiv(\tilde{M}^2+\mathbf{p}_m^2)^{1/2}$. The states of the nucleons in nuclear matter, w, are to be normalized by $w^{\dagger}w=1$. This is achieved by defining $w\equiv\sqrt{\tilde{M}/\tilde{E}}\times u$, which explains factors of $\tilde{M}/\tilde{E}$ in Eqs. (8)–(10).

The first term on the right-hand side (rhs) of Eq. (10)—the "kinetic energy"—is in more explicit form:

$$\frac{1}{A}\sum_{m\le k_F}\frac{M\tilde{M}+\mathbf{p}_m^2}{\tilde{E}_m}\ . \tag{12}$$

The single-particle energy is

$$\epsilon_m=\frac{\tilde{M}}{\tilde{E}_m}\langle m|\boldsymbol{\gamma}\cdot\mathbf{p}_m+M|m\rangle+U(m) \tag{13}$$

$$=\tilde{E}_m+U_V \tag{14}$$

$$=\tilde{E}_m-\tilde{M}+M+U_0\ . \tag{15}$$

III. RESULTS AND DISCUSSION

We construct three different OBE potentials, denoted by *A*, *B*, and *C* (see Appendixes B and C for all details), which are appropriate for the application to relativistic nuclear structure physics. It is not possible to use previous OBE models in a consistent way, since almost all earlier models use πNN vertices with pseudoscalar coupling. This coupling is inappropriate for the Dirac approach, since it leads to an unrealistically large attractive contribution.[40] Therefore, the potentials presented here use derivative (pseudovector) πNN coupling, which removes the problem. Another reason why earlier OBE potentials are inappropriate for our relativistic calculations is the fact that, in the past, almost exclusively either the BbS equation [see Eq. (A21) of Appendix A] or the nonrelativistic Lippmann-Schwinger equation has been used as a unitarizing equation. As mentioned, we use the Thompson equation [Appendix A, Eq. (A24)].

The parameters of the potentials and the predictions for the two-nucleon system are given in Appendix C. The main difference between the three potentials considered here is the strength of the tensor force as reflected in the predicted *D*-state probability of the deuteron, P_D. With $P_D=4.5\%$, potential *A* has the weakest tensor force. Potentials *B* and *C* predict 5.1% and 5.5%, respectively. It is well known[10] that the strength of the tensor force determines the location of the nuclear matter saturation point on the Coester band.[22] To find out the structure of the Coester band, predictions from more than one potential are needed.

All results presented in this paper are obtained either in the Bruckner-Hartree-Fock (BHF) or the Dirac-Brueckner-Hartree-Fock (DBHF) approximation; as mentioned before, occasionally, we will denote these two methods also as the "nonrelativistic" and the "relativistic" calculation, respectively.

The repulsive relativistic effect in nuclear matter as created by the DBHF method is shown in Fig. 2. In addition, in Table II we list the following quantities as a function of the Fermi momentum k_F: the energy per nucleon, $\mathcal{E}/A$, the ratio $\tilde{M}/M$, the single-particle scalar and vector potentials U_S and U_V, and the wound integral κ. (For the definition of κ and for explicit formulas appropriate for the momentum-space framework, see Sec. 5 of Ref. 7.) κ can be understood as the expansion parameter for the hole-line series.

As we mentioned already in Sec. II, the suppression of the σ contribution can be understood in simple terms by considering the covariant one-σ-exchange amplitude [Eq. (B6) of Appendix B] for $\mathbf{q}'=\mathbf{q}$ and $\lambda_i=\lambda_i'$ (as used in the Hartree approximation), in which case, because of the covariant normalization of the Dirac spinors [Eq. (B8)], the numerator becomes 1. Since the physical states of the nucleons in nuclear matter, w, are to be normalized by $w^{\dagger}w=1$, implying $w\equiv\sqrt{\tilde{M}/\tilde{E}}\times u$, the sigma (as any other) contribution gets the (scalar density) factor $(\tilde{M}/\tilde{E})^2$ [see second term on the rhs of Eq. (10)], which decreases with decreasing $\tilde{M}$ (i.e., increasing density). A corresponding consideration for the timelike (γ_0) component of ω exchange would lead to no changes for that contribution. However, because of the exchange term and correlations, there is a small enhancement of the repulsion created by the ω with density.

From the numbers given in Table II, it is seen that the relativistic effect on the energy per nucleon, $\Delta(\mathcal{E}/A)_{\rm rel}$ (i.e., the difference between the relativistic and nonrelativistic calculation), is well fitted by the ansatz

$$\Delta(\mathcal{E}/A)_{\rm rel}\approx 2\ \text{MeV}\times(\rho/\rho_0)^{8/3}\ , \tag{16}$$

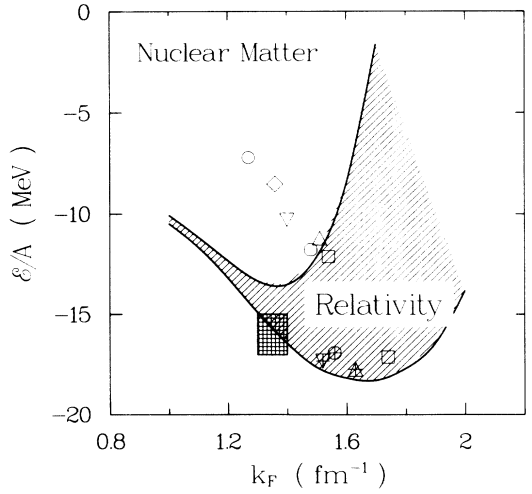

FIG. 2. Repulsive relativistic effect in nuclear matter as obtained in a Dirac-Brueckner-Hartree-Fock calculation using potential *B*. Saturation points from conventional calculations are displayed in the background (cf. Fig. 1). The checked rectangle represents the empirical value for nuclear matter saturation.

TABLE II. Results of a relativistic Dirac-Brueckner calculation in comparison to the corresponding nonrelativistic one using potential B. As a function of the Fermi momentum k_F, it is listed: the energy per nucleon $\mathcal{E}/A$, $\tilde{M}/M$, the single-particle scalar and vector potentials U_S and U_V, and the wound integral κ.

	Relativistic					Nonrelativistic			
k_F (fm^{-1})	$\mathcal{E}/A$ (MeV)	$\tilde{M}/M$	U_S (MeV)	U_V (MeV)	κ (%)	$\mathcal{E}/A$ (MeV)	$\tilde{M}/M$	U_0[a] (MeV)	κ (%)
0.8	−7.02	0.855	−136.2	104.0	23.1	−7.40	0.876	−33.0	26.5
0.9	−8.58	0.814	−174.2	134.1	18.8	−9.02	0.836	−41.0	21.6
1.0	−10.06	0.774	−212.2	164.2	16.1	−10.49	0.797	−49.0	18.5
1.1	−11.18	0.732	−251.3	195.5	12.7	−11.69	0.760	−58.1	14.2
1.2	−12.35	0.691	−290.4	225.8	11.9	−13.21	0.725	−68.5	12.9
1.3	−13.35	0.646	−332.7	259.3	12.5	−14.91	0.687	−80.5	13.1
1.35	−13.55	0.621	−355.9	278.4	13.0	−15.58	0.664	−86.8	13.2
1.4	−13.53	0.601	−374.3	293.4	13.8	−16.43	0.651	−93.2	13.5
1.5	−12.15	0.559	−413.6	328.4	14.4	−17.61	0.618	−106.1	13.0
1.6	−8.46	0.515	−455.2	371.0	15.8	−18.14	0.579	−119.4	12.7
1.7	−1.61	0.477	−491.5	415.1	18.4	−18.25	0.545	−133.2	13.2
1.8	+9.42	0.443	−523.4	463.6	21.9	−17.65	0.489	−147.2	14.3
1.9	25.26	0.418	−546.7	513.5	25.2	−16.41	0.480	−160.7	15.0
2.0	47.56	0.400	−563.6	568.6	27.5	−13.82	0.449	−173.6	15.3
2.1	77.40	0.381	−581.3	640.9	30.2	−9.70	0.411	−186.3	15.7
2.2	114.28	0.370	−591.2	723.5	33.3	−3.82	0.373	−198.1	16.3

[a] U_0 is to be compared to U_S+U_V; see Eq. (15).

which is suggested by an estimate by Keister and Wiringa.[54]

Furthermore, Table II shows that up to nuclear matter density, the wound integral κ is slightly smaller for the relativistic approach than for the nonrelativistic one. This implies that in this region the relativistic many-body scheme should be slightly better convergent. Beyond nuclear matter density, the situation is reversed. In addition, it is amusing to note that for all values of k_F the ratio $\tilde{M}/M$ is almost the same for the nonrelativistic and the relativistic approach. Low values for $\tilde{M}/M$ have often been criticized. However, they are not a consequence of the relativistic approach, but are due to the Brueckner-Hartree-Fock approximation. Higher-order corrections will enhance this quantity. For a recent discussion of the effective mass in relativistic and nonrelativistic approaches, see Ref. 55.

The representation of nucleons by Dirac spinors with an effective mass $\tilde{M}$ can be interpreted as taking virtual nucleon-antinucleon excitations in the many-body environment (many-body Z graphs) effectively into account.[56] This can be made plausible by expanding the spinor [Eq. (3)] in terms of (a complete set of) spinor solutions of the free Dirac equation, which will necessarily also include solutions representing negative-energy (antiparticle) states.[37]

In Table III we compare the contributions in various partial-wave states as obtained in a relativistic calculation to that from the corresponding nonrelativistic one. Detailed investigations have shown that the repulsive relativistic effect seen in that table for the P-wave contributions is essentially due to σ suppression together with a signature of spin-orbit force enhancement. The change of the $^1S_0$ contribution is so small, because of a cancellation of effects due to σ and ρ. Apart from σ reduction, the repulsive effect in $^3S_1$ is due to a suppression of the twice-iterated one-pion exchange for reasons quite analogous to the sigma suppression.

A comparison between relativistic and nonrelativistic Brueckner-Hartree-Fock calculations for all three potentials is shown in Fig. 3. For the nonrelativistic approach, the three saturation points are clearly on the Coester band. However, using the relativistic method, the saturation points are located on a new band which is shifted toward lower Fermi momenta (densities) and even meets the empirical area. This is a very desirable effect. The reason for this shift of the Coester band is the additional strongly density-dependent repulsion which the relativistic approach gives rise to. In Table IV the saturation points for the different potentials are given for the relativistic as well as the nonrelativistic calculation. In the relativistic case, the incompressibility of nuclear matter using potential B is about 250 MeV, which is in satisfactory agreement with the empirical value of 210±30 MeV.[57] Note that in the relativistic Walecka model, 540 MeV is obtained for the compression modulus.[33]

For completeness, we present in Table V the Landau parameters at various densities as obtained in a relativistic as well as a nonrelativistic nuclear matter calculation. Based on the nuclear matter G matrix, the effective particle-hole interaction at the Fermi surface is calculated and, multiplied by the density of states $k_F M/(\hbar^2\pi^2)$, parametrized by $F=f+f'\tau_1\tau_2+g\sigma_1\sigma_2+g'\sigma_1\sigma_2\tau_1\tau_2$. From an expansion of the parameters in terms of Legendre polynominals P_l, we give in Table V the coefficient for $l=0$. For more details and the empirical values, see Ref. 58. Note that the predictions for the Landau parameter f_0 is considerably improved in the relativistic calculation without deteriorating the other parameters. Sum rules require $f_0>-1$ at nuclear matter density.[53]

TABLE III. Partial-wave contributions to the energy in nuclear matter (in MeV) for a nonrelativistic and a relativistic calculation using potential *B*.

	$k_F=1.1$ fm^{-1}		$k_F=1.35$ fm^{-1}		$k_F=1.6$ fm^{-1}	
State	Nonrelativistic	Relativistic	Nonrelativistic	Relativistic	Nonrelativistic	Relativistic
$^1S_0$	−10.79	−11.18	−16.01	−16.42	−21.51	−20.36
$^3P_0$	−2.07	−1.48	−3.74	−1.34	−5.61	+2.17
$^1P_1$	1.73	1.77	3.25	3.45	5.33	6.08
$^3P_1$	4.71	5.27	9.77	12.33	17.69	26.65
$^3S_1$	−15.41	−14.16	−20.10	−17.10	−23.77	−17.03
$^3D_1$	0.59	0.57	1.38	1.29	2.64	2.25
$^1D_2$	−0.95	−0.91	−2.28	−2.01	−4.57	−3.39
$^3D_2$	−1.70	−1.62	−4.00	−3.56	−7.71	−5.99
$^3P_2$	−3.10	−2.92	−7.06	−6.28	−13.31	−10.73
$^3F_2$	−0.19	−0.18	−0.54	−0.44	−1.19	−0.67
$^1F_3$	0.32	0.31	0.80	0.75	1.60	1.40
$^3F_3$	0.56	0.55	1.51	1.43	3.20	2.87
$^3D_3$	−0.01	0.00	−0.03	0.00	−0.11	−0.02
$^3G_3$	0.06	0.06	0.20	0.18	0.49	0.41
$J\geq 4$	−0.34	−0.33	−1.07	−0.98	−2.57	−2.13
			Total			
Potential energy	−26.61	−24.25	−37.93	−28.72	−49.38	−18.51
Kinetic energy	14.91	13.07	22.35	15.16	31.23	10.05
Total energy	−11.69	−11.18	−15.58	−13.55	−18.14	−8.46

Finally, in Fig. 4, DBHF results are displayed for higher nuclear matter densities (using potential *A*). The nonrelativistic result is also shown (dashed line). The relativistic effects are growing dramatically for higher densities. On the other hand, the wound integral grows more rapidly in the relativistic case as compared to the nonrelativistic, (see Table II), which means that higher-order many-body corrections should be larger for the relativistic approach. Therefore, the theoretical curve carries an uncertainty which is growing with density. The error bars in Fig. 4 represent empirical information as deduced from pion production[59] (crosses) and transverse energy-momentum flow[60] (solid dots) in heavy-ion collisions. We mention that the error for these data may be underestimated. The shaded area ("Supernova") covers various assumptions for the equation of state used in the supernova calculations of Ref. 61. Again, the uncertainty may be larger than indicated by the shaded area. The empirical as well as the theoretical information displayed in Fig. 4 is rather preliminary and should be considered with caution; ultimately, there may be no discrepancy between the results from astrophysics and heavy-ion physics. At present, this issue is under major investigation by several groups.

More nuclear matter results are tabulated in Appendix C.

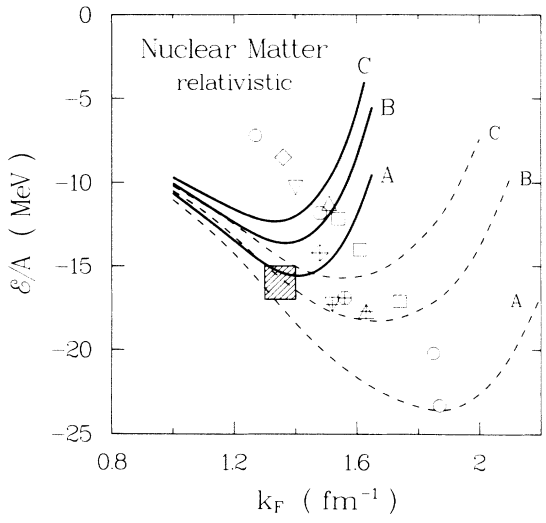

FIG. 3. Results from calculations with a family of relativistic potentials revealing a new Coester band which meets the empirical area; solid lines: relativistic; dashed lines: nonrelativistic calculations. For comparison, saturation points from conventional calculations are displayed in the background (cf. Fig. 1). The shaded square denotes the empirical value for nuclear matter saturation.

IV. SUMMARY AND OUTLOOK

In this paper we have presented the formalism for a relativistic approach to nuclear structure which is based upon a relativistic extension of Brueckner theory. The essential idea of this approach is to use the Dirac equation for the single-particle motion. The nucleon self-energy in nuclear matter obtained in this framework consists of a large (attractive) scalar and (repulsive) vector field. The size of these potentials (several hundred MeV) motivates the use of the Dirac equation.

Furthermore, we have constructed relativistic meson-exchange potentials appropriate for this approach. We use the one-boson-exchange (OBE) model including the six nonstrange bosons with masses below 1 GeV/c^2, π, η, σ, δ, ω, and ρ. The potentials describe low-energy NN scattering and the properties of the deuteron quantitatively. Thus they are suitable for (parameter-free) micro-

TABLE IV. Energy per particle, $\mathcal{E}/A$, Fermi momentum k_F, and compression modulus K at saturation for nuclear matter with and without relativistic effects.

	Relativistic			Nonrelativistic		
Potential	$\mathcal{E}/A$ (MeV)	k_F (fm^{-1})	K (MeV)	$\mathcal{E}/A$ (MeV)	k_F (fm^{-1})	K (MeV)
A	−15.59	1.40	290	−23.55	1.85	204
B	−13.60	1.37	249	−18.30	1.66	160
C	−12.26	1.32	185	−15.75	1.54	143

scopic nuclear structure calculations. Apart from the usual interaction Lagrangians for heavy mesons, these potentials apply the pseudovector (gradient) coupling for the πNN (and ηNN) vertex. For a relativistic approach, it is necessary to apply this coupling for the pseudoscalar mesons, since the commonly used pseudoscalar coupling leads to unrealistically attractive contributions.

The consideration of the two-nucleon system is based upon the relativistic three-dimensional reduction of the Bethe-Salpeter equation introduced by Thompson. We derive and present the Thompson equation for an arbitrary frame. In two-nucleon scattering this equation is applied in the two-nucleon c.m. system, while in nuclear matter the nuclear matter rest frame is used. Thus we calculate the nuclear matter G matrix directly in the nuclear matter rest frame in which it is needed to obtain the energy of the many-body system. The advantage of this method is that, in the nuclear medium, the rather involved and tedious transformation between the two-nucleon c.m. frame and the nuclear matter rest frame is avoided.

Using the framework outlined, the properties of nuclear matter are calculated in the Dirac-Brueckner-Hartree-Fock (DBHF) approximation. The single-particle scalar and vector fields as well as the single-particle wave functions (Dirac spinors) are determined fully self-consistently. The strong attractive scalar field leads to a reduction of the nucleon mass in the medium, which increases with density. One consequence of this is a suppression of the (attractive) scalar-boson exchange. This strongly density-dependent effect improves nuclear saturation considerably such that the empirical saturation energy and density can be explained correctly. Our calculations include also the saturation mechanisms of conventional (nonrelativistic) many-body theory (i.e., Pauli and dispersion effects). The predictions for the compression modulus of nuclear matter as well as the Landau parameters are in satisfactory agreement with empirical information.

The application of the relativistic framework, presented in this paper, to finite systems will be studied in a forthcoming paper.[45]

The formalism, the potentials, and the results of this paper may serve as a sound basis and as a well-defined starting point for various relativistic nuclear structure studies. In fact, it is desirable that, using the relativistic microscopic framework outlined in this paper, systematic investigations are performed also in other areas of nuclear structure physics, such as the ground state of finite nuclear, excited states of nuclei, and nucleon-nucleus scattering. Only a systematic study of the main phenomena of nuclear structure physics will give insight into the important question as to whether or not the relativistic approach is superior to the nonrelativistic one. The answer to this question is crucial with regard to the general relevance and credibility of relativistic approaches in nuclear physics.

In spite of the success of the present calculations, several critical questions can be raised. First, there will be contributions of higher order in the conventional hole-line expansion. For nonrelativistic Brueckner theory, Day found an increase in the binding energy per nucleon of 5–7 MeV from the three- and four-hole line contributions. Note that in the work of Day the standard choice ("gap" choice) for the single-particle potential is used (this is true for all results displayed in Table I and Fig. 1). However, in the calculations of our work the continuous choice for the single-particle potential [Eq.

TABLE V. Landau parameters at various densities from a nonrelativistic and a relativistic nuclear matter calculation using potential B.

k_F (fm^{-1})	Density		f_0	f_0'	g_0	g_0'
1.0	$0.4\rho_0$	relativistic	−1.37	0.57	0.22	0.66
		nonrelativistic	−1.50	0.62	0.16	0.66
1.35	ρ_0	relativistic	−0.79	0.35	0.28	0.67
		nonrelativistic	−1.27	0.38	0.15	0.67
1.7	$2\rho_0$	relativistic	0.56	0.29	0.36	0.68
		nonrelativistic	−0.99	0.20	0.14	0.69
2.0	$3.25\rho_0$	relativistic	2.21	0.37	0.38	0.69
		nonrelativistic	−0.71	0.09	0.11	0.71
	(empirical)		(0±0.2)	(≈0.8)	(≈0.2)	(≈0.9)

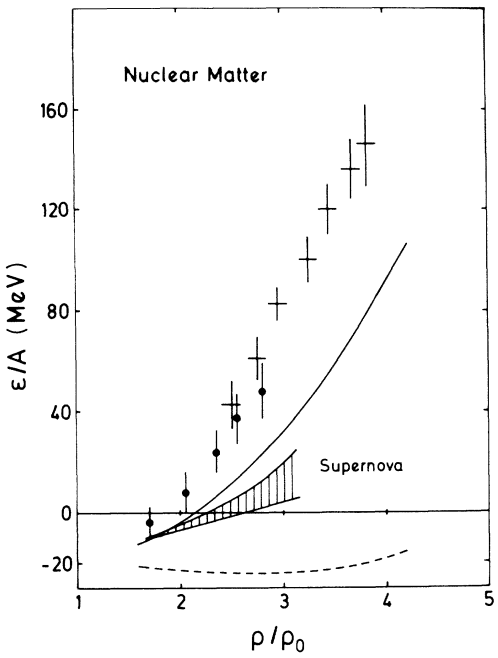

FIG. 4. Dirac-Brueckner results for nuclear matter (solid line) at higher densities using potential A. The empirical points are taken from Refs. 59 and 60. The shaded area shows different equations of state as used in supernova calculations (Ref. 61). The dashed line is the prediction by the nonrelativistic Brueckner calculation (using potential A). (ρ_0 denotes the nuclear matter saturation density.)

(9)] is applied. In the two-hole line approximation, this choice leads to about 4 MeV more binding energy per nucleon as compared to the gap choice. Investigations by the Liège group[62] suggest that a lowest-order calculation with the continuous choice effectively includes the three-hole line contributions. In light of this result, the contributions of higher order in the hole-line expansion, missing in our work, may be believed to be small.

In a recent study, a special class of ring diagrams has been summed up to infinite orders using the relativistic G matrix of the present paper. Only a minor change of the present DBHF result is found,[63] which, however, further improves the saturation density.

Second, one may question the OBE model. The weakest part of that model is the scalar isoscalar σ boson. However, as mentioned, Dirac-Brueckner calculations have also been performed with more realistic meson models, in which the fictitious σ is replaced by an explicit description of the 2π-exchange contribution to the NN interaction. In those calculations it is found that the relativistic effect comes out almost exactly the same as in the OBE model.[44] This is not too surprising since it has been known for a long time that the 2π-exchange part of the nuclear potential is well approximated by the exchange of a single scalar isoscalar boson of intermediate mass.

One may also criticize that the present approach is restricted to positive-energy nucleons. At a first glance, this may appear rather inconsistent in a relativistic framework. However, calculations done for two-nucleon scattering have shown that the contributions from virtual antinucleon intermediate states (pair terms) are extremely small (when the pseudovector coupling is used for the pion).[64,65] Thus the medium effects on this small contribution will be even smaller. Still, a calculation which treats nucleons and antinucleons on an equal footing would be more consistent than our present approach; it represents an interesting project for the future.

Since higher orders in the hole-line expansion are attractive, while corrections from the Dirac sea (of antinucleons) have (as far as calculations exist) yielded additional repulsion,[43] cancellations may occur between many-body contributions missing in the present approach. Thus it is not unlikely that DBHF may ultimately turn out to be a reasonable approximation to this very complex (relativistic) many-body problem. However, in the present stage the latter remark is just speculation; in fact, we like to stress that the agreement between experiment and theory (e.g., for case A in Fig. 3) is not very relevant from a basic point of view.

On a more fundamental level, one may raise the critical question how serious and reliable the meson model is. Note that the relativistic effects obtained in Dirac approaches are intimately linked to the meson model for the nuclear force. In the meson-exchange model for the NN interaction, the isoscalar vector meson ω and the isoscalar σ boson provide the largest contributions. In our many-body framework, they are responsible for the large effective scalar and vector fields obtained for the single-particle potential (nucleon self-energy) in the many-body system. Assuming that quantum chromodynamics (QCD) is the fundamental theory of strong interactions, one of the greatest challenges we have to face is the simple question: Why do these meson models work so well for two as well as many nucleons?

This work was supported in part by the U.S. National Science Foundation (through the Idaho-EPSCoR Program under Grant No. RII-8902065, under Grant No. PHY-8911040, and through the San Diego Supercomputer Center) and by the NATO Scientific Affairs Division (Collaborative Research Grant No. 0147/89).

APPENDIX A: RELATIVISTIC THREE-DIMENSIONAL EQUATIONS

Two-nucleon scattering is described covariantly by the Bethe-Salpeter (BS) equation.[48] In operator notation it may be written as

$$\mathcal{M}=\mathcal{V}+\mathcal{V}\mathcal{G}\mathcal{M}\ , \tag{A1}$$

with $\mathcal{M}$ the invariant amplitude for the two-nucleon scattering process, $\mathcal{V}$ the sum of all connected two-particle irreducible diagrams, and $\mathcal{G}$ the relativistic two-nucleon propagator. As this four-dimensional integral equation is very difficult to solve,[66] so-called three-dimensional reductions have been proposed, which are more amenable to numerical solution. Furthermore, it has been shown by Gross[67] that the full BS equation in ladder approximation does not generate the desired one-body equation in the one-body limit (i.e., when one of the particles becomes very massive) in contrast to a large

family of three-dimensional quasipotential equations. These approximations to the BS equation are also covariant and satisfy relativistic elastic unitarity. However, the three-dimensional reduction is not unique, and in principal infinitely many choices exist.[68] Typically, they are derived by replacing Eq. (A1) by two coupled equations:

$$\mathcal{M}=\mathcal{W}+\mathcal{W}g\mathcal{M}\ , \tag{A2}$$

and

$$\mathcal{W}=\mathcal{V}+\mathcal{V}(\mathcal{G}-g)\mathcal{W}\ , \tag{A3}$$

where g is a covariant three-dimensional propagator with the same elastic unitarity cut as $\mathcal{G}$ in the physical region. In general, the second term on the rhs of Eq. (A3) is dropped to arrive at a substantial simplification of the problem.

Explicitly, we can write the BS equation for an arbitrary frame (notation and conventions of Ref. 46):

$$\mathcal{M}(q',q|P)=\mathcal{V}(q',q|P)+\int d^4k\ \mathcal{V}(q',k|P)\mathcal{G}(k|P)\mathcal{M}(k,q|P)\ , \tag{A4}$$

with

$$\mathcal{G}(k|P)=\frac{i}{(2\pi)^4}\frac{1}{(\frac{1}{2}\not{P}+\not{k}-M+i\epsilon)^{(1)}}\times\frac{1}{(\frac{1}{2}\not{P}-\not{k}-M+i\epsilon)^{(2)}} \tag{A5}$$

$$=\frac{i}{(2\pi)^4}\left[\frac{\frac{1}{2}\not{P}+\not{k}+M}{(\frac{1}{2}P+k)^2-M^2+i\epsilon}\right]^{(1)}\times\left[\frac{\frac{1}{2}\not{P}-\not{k}+M}{(\frac{1}{2}P-k)^2-M^2+i\epsilon}\right]^{(2)}\ , \tag{A6}$$

where q, k, and q' are the initial, intermediate, and final relative four-momenta, respectively [with, e.g., $k=(k_0,\mathbf{k})$], and $P=(P_0,\mathbf{P})$ is the total four-momentum; $\not{k}=\gamma^\mu k_\mu$. The superscripts refer to particles (1) and (2). In general, we suppress spin (or helicity) and isospin indices.

$\mathcal{G}$ and g have the same discontinuity across the right-hand cut, if

$$\mathrm{Im}\mathcal{G}(k|P)=-\frac{2\pi^2}{(2\pi)^4}(\tfrac{1}{2}\not{P}+\not{k}+M)^{(1)}(\tfrac{1}{2}\not{P}-\not{k}+M)^{(2)}\delta^{(+)}[(\tfrac{1}{2}P+k)^2-M^2]\delta^{(+)}[(\tfrac{1}{2}P-k)^2-M^2]$$
$$=\mathrm{Im}g(k|P)\ , \tag{A7}$$

with $\delta^{(+)}$ indicating that only the positive-energy root of the argument of the δ function is to be included. From this follows easily

$$\mathrm{Im}g(k|P)=-\frac{1}{8\pi^2}(\tfrac{1}{2}\not{P}+\not{k}+M)^{(1)}(\tfrac{1}{2}\not{P}-\not{k}+M)^{(2)}\frac{\delta(\frac{1}{2}P_0+k_0-E_{(1/2)\mathbf{P}+\mathbf{k}})\delta(\frac{1}{2}P_0-k_0-E_{(1/2)\mathbf{P}-\mathbf{k}})}{4E_{(1/2)\mathbf{P}+\mathbf{k}}E_{(1/2)\mathbf{P}-\mathbf{k}}}\ , \tag{A8}$$

with $E_{(1/2)\mathbf{P}\pm\mathbf{k}}\equiv[M^2+(\frac{1}{2}\mathbf{P}\pm\mathbf{k})^2]^{1/2}$. Using the equality

$$\delta(\tfrac{1}{2}P_0+k_0-E_{(1/2)\mathbf{P}+\mathbf{k}})\delta(\tfrac{1}{2}P_0-k_0-E_{(1/2)\mathbf{P}-\mathbf{k}})=\delta(P_0-E_{(1/2)\mathbf{P}+\mathbf{k}}-E_{(1/2)\mathbf{P}-\mathbf{k}})\delta(k_0-\tfrac{1}{2}E_{(1/2)\mathbf{P}+\mathbf{k}}+\tfrac{1}{2}E_{(1/2)\mathbf{P}-\mathbf{k}})\ , \tag{A9}$$

the imaginary part of the propagator $g(k|P)$ can now be written:

$$\mathrm{Im}g(k|P)=-\frac{1}{8\pi^2}\frac{M^2}{E_{(1/2)\mathbf{P}+\mathbf{k}}E_{(1/2)\mathbf{P}-\mathbf{k}}}\times\Lambda_+^{(1)}(\tfrac{1}{2}\mathbf{P}+\mathbf{k})\Lambda_+^{(2)}(\tfrac{1}{2}\mathbf{P}-\mathbf{k})\times\delta(P_0-E_{(1/2)\mathbf{P}+\mathbf{k}}-E_{(1/2)\mathbf{P}-\mathbf{k}})\times\delta(k_0-\tfrac{1}{2}E_{(1/2)\mathbf{P}+\mathbf{k}}+\tfrac{1}{2}E_{(1/2)\mathbf{P}-\mathbf{k}})\ , \tag{A10}$$

where

$$\Lambda_+^{(i)}(\mathbf{p})=\left[\frac{\gamma^0E_{\mathbf{p}}-\boldsymbol{\gamma}\cdot\mathbf{p}+M}{2M}\right]^{(i)} \tag{A11}$$

$$=\sum_{\lambda_i}u(\mathbf{p},\lambda_i)\bar{u}(\mathbf{p},\lambda_i) \tag{A12}$$

represents the positive-energy projection operator for nucleon i ($i=1,2$) with $u(\mathbf{p})$ a positive-energy Dirac spinor of momentum $\mathbf{p}$; λ_i denotes either the helicity or the spin projection of the respective nucleon, and $E_{\mathbf{p}}=(M^2+\mathbf{p}^2)^{1/2}$. The projection operators imply that contributions involving virtual antinucleon intermediate states ("pair terms") are suppressed. It has been shown in Refs. 64 and 65 that these contributions are small when the pseudovector coupling is used for the pion.

Note that $\mathrm{Im}g(k|P)$ is covariant, since $\mathrm{Im}g(k|P)=\mathrm{Im}\mathcal{G}(k|P)$.

Using $\delta(P_0-E)=2E\delta(s-E^2+\mathbf{P}^2)$, where $E=E_{(1/2)\mathbf{P}+\mathbf{k}}+E_{(1/2)\mathbf{P}-\mathbf{k}}$ and $s=P^2=P_0^2-\mathbf{P}^2$, Eq. (A10) can be rewritten as

$$\mathrm{Img}(k|s)=-\frac{M^2}{8\pi^2}\frac{2(E_{(1/2)\mathbf{P}+\mathbf{k}}+E_{(1/2)\mathbf{P}-\mathbf{k}})}{E_{(1/2)\mathbf{P}+\mathbf{k}}E_{(1/2)\mathbf{P}-\mathbf{k}}}\times\Lambda_+^{(1)}(\tfrac{1}{2}\mathbf{P}+\mathbf{k})\Lambda_+^{(2)}(\tfrac{1}{2}\mathbf{P}-\mathbf{k})\times\delta[s-(E_{(1/2)\mathbf{P}+\mathbf{K}}+E_{(1/2)\mathbf{P}-\mathbf{k}})^2+\mathbf{P}^2]\times\delta(k_0-\tfrac{1}{2}E_{(1/2)\mathbf{P}+\mathbf{k}}+\tfrac{1}{2}E_{(1/2)\mathbf{P}-\mathbf{k}})\ . \tag{A13}$$

Knowing its imaginary part, we construct $g(k|s)$ by a dispersion integral

$$g(k|s)=\frac{1}{\pi}\int_{4M^2}^{\infty}\frac{ds'}{s'-s-i\epsilon}\mathrm{Img}(k|s')\ . \tag{A14}$$

Inserting Eq. (A13) in Eq. (A14) and integrating, we obtain

$$g(k|P)=-\frac{M^2}{(2\pi)^3}\frac{2(E_{(1/2)\mathbf{P}+\mathbf{k}}+E_{(1/2)\mathbf{P}-\mathbf{k}})}{E_{(1/2)\mathbf{P}+\mathbf{k}}E_{(1/2)\mathbf{P}-\mathbf{k}}}\frac{\Lambda_+^{(1)}(\frac{1}{2}\mathbf{P}+\mathbf{k})\Lambda_+^{(2)}(\frac{1}{2}\mathbf{P}-\mathbf{k})}{(E_{(1/2)\mathbf{P}+\mathbf{k}}+E_{(1/2)\mathbf{P}-\mathbf{k}})^2-\mathbf{P}^2-s-i\epsilon}\delta(k_0-\tfrac{1}{2}E_{(1/2)\mathbf{P}+\mathbf{k}}+\tfrac{1}{2}E_{(1/2)\mathbf{P}-\mathbf{k}})\ . \tag{A15}$$

This three-dimensional propagator is known as the Blankenbecler-Sugar (BbS) choice.[49,69] By construction, the propagator g has the same discontinuity across the right-hand cut as $\mathcal{G}$; therefore, it preserves the unitarity relation satisfied by $\mathcal{M}$.

Using the angle averages $(\frac{1}{2}\mathbf{P}\pm\mathbf{k})^2\approx\frac{1}{4}\mathbf{P}^2+\mathbf{k}^2$ and $(\frac{1}{2}\mathbf{P}\pm\mathbf{q})^2\approx\frac{1}{4}\mathbf{P}^2+\mathbf{q}^2$, which should be a very good approximation, Eq. (A15) assumes the much simpler form

$$g(k|P)=\frac{1}{(2\pi)^3}\frac{M^2}{E_{(1/2)\mathbf{P}+\mathbf{k}}}\frac{\Lambda_+^{(1)}(\frac{1}{2}\mathbf{P}+\mathbf{k})\Lambda_+^{(2)}(\frac{1}{2}\mathbf{P}-\mathbf{k})}{E_{(1/2)\mathbf{P}+\mathbf{q}}^2-E_{(1/2)\mathbf{P}+\mathbf{k}}^2+i\epsilon}\delta(k_0)\ , \tag{A16}$$

where we used $s=4E_{(1/2)\mathbf{P}+\mathbf{q}}^2-\mathbf{P}^2$.

Assuming $\mathcal{W}=\mathcal{V}$, the reduced Bethe-Salpeter equation [Eq. (A1)] is obtained in explicit form by replacing in Eq. (A4) $\mathcal{G}$ by g of Eq. (A16), yielding

$$\mathcal{M}(\mathbf{q}',\mathbf{q}|\mathbf{P})=\mathcal{V}(\mathbf{q}',\mathbf{q}|\mathbf{P})+\int\frac{d^3k}{(2\pi)^3}\mathcal{V}(\mathbf{q}',\mathbf{k}|\mathbf{P})\frac{M^2}{E_{(1/2)\mathbf{P}+\mathbf{k}}}\frac{\Lambda_+^{(1)}(\frac{1}{2}\mathbf{P}+\mathbf{k})\Lambda_+^{(2)}(\frac{1}{2}\mathbf{P}-\mathbf{k})}{E_{(1/2)\mathbf{P}+\mathbf{q}}^2-E_{(1/2)\mathbf{P}+\mathbf{k}}^2+i\epsilon}\mathcal{M}(\mathbf{k},\mathbf{q}|\mathbf{P})\ , \tag{A17}$$

in which both nucleons in intermediate states are equally far off their mass shell.

Taking matrix elements between positive-energy spinors yields an equation for the scattering amplitude in an arbitrary frame:

$$\mathcal{T}(\mathbf{q}',\mathbf{q}|\mathbf{P})=V(\mathbf{q}',\mathbf{q})+\int\frac{d^3k}{(2\pi)^3}V(\mathbf{q}',\mathbf{k})\frac{M^2}{E_{(1/2)\mathbf{P}+\mathbf{k}}}\frac{1}{E_{(1/2)\mathbf{P}+\mathbf{q}}^2-E_{(1/2)\mathbf{P}+\mathbf{k}}^2+i\epsilon}\mathcal{T}(\mathbf{k},\mathbf{q}|\mathbf{P})\ , \tag{A18}$$

where we used

$$\begin{aligned}&\bar{u}_1(\tfrac{1}{2}\mathbf{P}+\mathbf{q}')\bar{u}_2(\tfrac{1}{2}\mathbf{P}-\mathbf{q}')\mathcal{V}(\mathbf{q}',\mathbf{q}|\mathbf{P})u_1(\tfrac{1}{2}\mathbf{P}+\mathbf{q})u_2(\tfrac{1}{2}\mathbf{P}-\mathbf{q})\\&\quad=\bar{u}_1(\mathbf{q}')\bar{u}_2(-\mathbf{q}')\mathcal{V}(\mathbf{q}',\mathbf{q})u_1(\mathbf{q})u_2(-\mathbf{q})\\&\quad\equiv V(\mathbf{q}',\mathbf{q})\ ,\end{aligned} \tag{A19}$$

since this is a Lorentz scalar. An analogous statement applies to $\mathcal{T}$. Calculations of nuclear matter and of finite nuclei are performed in the rest frame of these systems. Thus Eq. (A18) with the necessary medium modifications would be appropriate for the evaluation of the nuclear matter reaction (G) matrix.

In the two-nucleon c.m. frame (i.e., for $\mathbf{P}=0$), the BbS propagator [Eq. (A15)] reduces to

$$g(\mathbf{k},s)=\frac{1}{(2\pi)^3}\frac{M^2}{E_{\mathbf{k}}}\frac{\Lambda_+^{(1)}(\mathbf{k})\Lambda_+^{(2)}(-\mathbf{k})}{\frac{1}{4}s-E_{\mathbf{k}}^2+i\epsilon}\delta(k_0)\ , \tag{A20}$$

which implies the scattering equation

$$\mathcal{T}(\mathbf{q}',\mathbf{q})=V(\mathbf{q}',\mathbf{q})+\int\frac{d^3k}{(2\pi)^3}V(\mathbf{q}',\mathbf{k})\frac{M^2}{E_k}\frac{1}{\mathbf{q}^2-\mathbf{k}^2+i\epsilon}\mathcal{T}(\mathbf{k},\mathbf{q})\ . \tag{A21}$$

Two-nucleon scattering is considered most conveniently in the two-nucleon c.m. frame; thus, for calculations of free-space two-nucleon scattering in the BbS approximation, one would use Eq. (A21).

The BbS propagator is the most widely used approximation. Another choice, which has been frequently applied, is the version suggested by Thompson.[47] The manifestly covariant form of Thompson's propagator is the same as Eq. (A14), but with $\int_{4M^2}^{\infty}ds'/(s'-s-i\epsilon)$ replaced by $\int_{2M}^{\infty}d\sqrt{s'}/(\sqrt{s'}-\sqrt{s}-i\epsilon)$. After taking the angle average for $|\frac{1}{2}\mathbf{P}\pm\mathbf{k}|$ and $|\frac{1}{2}\mathbf{P}\pm\mathbf{q}|$, this propagator reads

$$g(k|P)=\frac{1}{(2\pi)^3}\frac{M^2}{E_{\mathbf{k}}E_{(1/2)\mathbf{P}+\mathbf{k}}} \times\frac{\Lambda_+^{(1)}(\frac{1}{2}\mathbf{P}+\mathbf{k})\Lambda_+^{(2)}(\frac{1}{2}\mathbf{P}-\mathbf{k})}{2E_{\mathbf{q}}-2E_{\mathbf{k}}+i\epsilon}\delta(k_0)\ . \quad \text{(A22)}$$

The equation for the scattering amplitude in an arbitrary frame is

$$\mathcal{T}(\mathbf{q}',\mathbf{q}|\mathbf{P})=V(\mathbf{q}',\mathbf{q}) +\int\frac{d^3k}{(2\pi)^3}V(\mathbf{q}',\mathbf{k})\frac{M^2}{E_{\mathbf{k}}E_{(1/2)\mathbf{P}+\mathbf{k}}} \times\frac{1}{2E_{\mathbf{q}}-2E_{\mathbf{k}}+i\epsilon}\mathcal{T}(\mathbf{k},\mathbf{q}|\mathbf{P})\ . \quad \text{(A23)}$$

For calculations in the rest frame of nuclear matter or finite nuclei, this equation, together with the necessary medium modifications ($M\mapsto\tilde{M}$, Pauli projector Q), is appropriate [see Eq. (6)]. In our actual calculations in nuclear matter, we replace $E_{\mathbf{k}}$ by $E_{(1/2)\mathbf{P}+\mathbf{k}}$ and $E_{\mathbf{q}}$ by $E_{(1/2)\mathbf{P}+\mathbf{q}}$ in the denominator of Eq. (A23) [see Eq. (6)]. This replacement makes possible an interpretation of the energy denominator in terms of differences between single-particle energies which are typically defined in the rest frame of the many-body system. This allows for a consistent application of this equation in nuclear matter *and* finite nuclei. The change of the numerical results by this replacement is negligibly small (less than 0.1 MeV for the energy per nucleon at nuclear matter density), since the factor $M^2/E_{\mathbf{k}}E_{(1/2)\mathbf{P}+\mathbf{k}}$ is slightly reduced, while the term $(2E_{\mathbf{q}}-2E_{\mathbf{k}}+i\epsilon)^{-1}$ is slightly enhanced.

Applying exactly the same potential, we have also made a quantitative comparison between our method and the one used by ter Haar and Malfliet[41] (which is essentially the same as that described by Horowitz and Serot[43]) where the Brueckner G matrix is first calculated in the two-nucleon c.m. system and then transformed to the rest frame: The numerical results agree within less than 0.5 MeV for the energy per nucleon at nuclear matter density.[70]

In the two-nucleon c.m. frame ($\mathbf{P}=0$), the Thompson equation is

$$\mathcal{T}(\mathbf{q}',\mathbf{q})=V(\mathbf{q}',\mathbf{q})+\int\frac{d^3k}{(2\pi)^3}V(\mathbf{q}',\mathbf{k})\frac{M^2}{E_{\mathbf{k}}^2} \times\frac{1}{2E_{\mathbf{q}}-2E_{\mathbf{k}}+i\epsilon}\mathcal{T}(\mathbf{k},\mathbf{q})\ . \quad \text{(A24)}$$

This equation is useful for free-space two-nucleon scattering. In the calculations of this paper, always Thompson's equations are used.

Since both nucleons are equally off-shell in the BbS or Thompson equation, the exchanged bosons transfer three-momentum only; i.e., the meson propagator is (for a scalar exchange)

$$\frac{i}{-(\mathbf{q}'-\mathbf{q})^2-m_\alpha^2}\ ; \quad \text{(A25)}$$

this is also referred to as a static (or nonretarded) propagator.

Many more choices for g have been suggested in the literature. For most of the other choices, the three-dimensional two-nucleon propagator is either of the BbS or the Thompson form. However, there may be differences in the δ function in Eqs. (A20) and (A22). For example, Schierholz[20] and Erkelenz[51] propose $\delta(k_0+\frac{1}{2}\sqrt{s}-E_k)$, restricting one particle to its mass shell. It implies the meson propagator

$$\frac{i}{(E_{\mathbf{q}'}-E_{\mathbf{q}})^2-(\mathbf{q}'-\mathbf{q})^2-m_\alpha^2}\ . \quad \text{(A26)}$$

However, it has been shown[71] (see also Appendix E.1 of Ref. 72) that the term $(E_{\mathbf{q}'}-E_{\mathbf{q}})^2$ in this propagator has an effect which is opposite to the one obtained when treating meson retardation properly. Also, the medium effect on meson propagation in nuclear matter which, when calculated correctly, is repulsive,[50] comes out attractive when using the form Eq. (A26).[52] Thus, in spite of its suggestive appearance and in spite of early beliefs, the meson propagator [Eq. (A26)] has nothing to do with genuine meson retardation and, therefore, should be discarded. This remark applies to the scattering of two particles of equal mass. If one particle is much heavier than the other one, it may, however, be appropriate to put one particle (namely, the more massive one) on its mass shell.

A thorough discussion of the Bethe-Salpeter equation and/or a systematic study of a large family of possible relativistic three-dimensional reductions can be found in Refs. 73–75. Tjon and co-workers have compared results obtained by solving the full four-dimensional Bethe-Salpeter equation applying a full set of OBE diagrams with those from the BbS and some other three-dimensional equations; for BbS they find only small differences as compared to full BS.[64,65] This is also true for the Thompson choice, since it differs little from BbS.

APPENDIX B: INTERACTION LAGRANGIANS AND OBE AMPLITUDES

We use the following Lagrangians for meson-nucleon coupling:

$$\mathcal{L}_{pv}=-\frac{f_{ps}}{m_{ps}}\bar{\psi}\gamma^5\gamma^\mu\psi\partial_\mu\varphi^{(ps)}\ , \quad \text{(B1)}$$

$$\mathcal{L}_s=+g_s\bar{\psi}\psi\varphi^{(s)}\ , \quad \text{(B2)}$$

$$\mathcal{L}_v=-g_v\bar{\psi}\gamma^\mu\psi\varphi_\mu^{(v)}-\frac{f_v}{4M}\bar{\psi}\sigma^{\mu\nu}\psi(\partial_\mu\varphi_\nu^{(v)}-\partial_\nu\varphi_\mu^{(v)})\ , \quad \text{(B3)}$$

with ψ the nucleon and $\varphi_{(\mu)}^{(\alpha)}$ the meson fields (notation and conventions as in Ref. 46). For isospin-1 mesons, $\varphi^{(\alpha)}$ is to be replaced by $\tau\cdot\varphi^{(\alpha)}$, with τ^l ($l=1,2,3$) the usual Pauli matrices. ps, pv, s, and v denote pseudoscalar, pseudovector, scalar, and vector coupling/field, respectively.

The one-boson-exchange potential (OBEP) is defined as a sum of one-particle-exchange amplitudes of certain bosons with given mass and coupling. We use the six non-strange bosons with masses below 1 GeV/c^2. Thus

$$V_{\rm OBEP}=\sum_{\alpha=\pi,\eta,\rho,\omega,\delta,\sigma} V_\alpha^{\rm OBE}\ , \tag{B4}$$

with π and η pseudoscalar, σ and δ scalar, and ρ and ω vector particles. The contributions from the isovector bosons π, δ, and ρ are to be multiplied by a factor of $\tau_1\cdot\tau_2$.

The Lagrangians mentioned lead to the following (off-shell) OBE amplitudes:[76]

$$\begin{aligned}
&\langle \mathbf{q}'\lambda_1'\lambda_2'|V_{pv}^{\rm OBE}|\mathbf{q}\lambda_1\lambda_2\rangle \\
&\quad=\frac{f_{ps}^2}{m_{ps}^2}\bar u(\mathbf{q}',\lambda_1')\gamma^5\gamma^\mu i(q'-q)_\mu u(\mathbf{q},\lambda_1)\bar u(-\mathbf{q}',\lambda_2')\gamma^5\gamma^\mu i(q'-q)_\mu u(-\mathbf{q},\lambda_2)/[(\mathbf{q}'-\mathbf{q})^2+m_{ps}^2] \\
&\quad=f_{ps}^2\frac{4M^2}{m_{ps}^2}\{\bar u(\mathbf{q}',\lambda_1')\gamma^5 u(\mathbf{q},\lambda_1)\bar u(-\mathbf{q}',\lambda_2')\gamma^5 u(-\mathbf{q},\lambda_2) \\
&\qquad+[(E'-E)/(2M)]^2\bar u(\mathbf{q}',\lambda_1')\gamma^5\gamma^0 u(\mathbf{q},\lambda_1)\bar u(-\mathbf{q}',\lambda_2')\gamma^5\gamma^0 u(-\mathbf{q},\lambda_2) \\
&\qquad+[(E'-E)/(2M)][\bar u(\mathbf{q}',\lambda_1')\gamma^5 u(\mathbf{q},\lambda_1)\bar u(-\mathbf{q}',\lambda_2')\gamma^5\gamma^0 u(-\mathbf{q},\lambda_2) \\
&\qquad\qquad+\bar u(\mathbf{q}',\lambda_1')\gamma^5\gamma^0 u(\mathbf{q},\lambda_1)\bar u(-\mathbf{q}',\lambda_2')\gamma^5 u(-\mathbf{q},\lambda_2)]\}/[(\mathbf{q}'-\mathbf{q})^2+m_{ps}^2]
\end{aligned} \tag{B5}$$

$$\langle \mathbf{q}'\lambda_1'\lambda_2'|V_s^{\rm OBE}|\mathbf{q}\lambda_1\lambda_2\rangle=-g_s^2\bar u(\mathbf{q}',\lambda_1')u(\mathbf{q},\lambda_1)\bar u(-\mathbf{q}',\lambda_2')u(-\mathbf{q},\lambda_2)/[(\mathbf{q}'-\mathbf{q})^2+m_s^2] \tag{B6}$$

$$\begin{aligned}
\langle \mathbf{q}'\lambda_1'\lambda_2'|V_v^{\rm OBE}|\mathbf{q}\lambda_1\lambda_2\rangle&=\left[g_v\bar u(\mathbf{q}',\lambda_1')\gamma_\mu u(\mathbf{q},\lambda_1)+\frac{f_v}{2M}\bar u(\mathbf{q}',\lambda_1')\sigma_{\mu\nu}i(q'-q)^\nu u(\mathbf{q},\lambda_1)\right] \\
&\quad\times\left[g_v\bar u(-\mathbf{q}',\lambda_2')\gamma^\mu u(-\mathbf{q},\lambda_2)-\frac{f_v}{2M}\bar u(-\mathbf{q}',\lambda_2')\sigma^{\mu\nu}i(q'-q)_\nu u(-\mathbf{q},\lambda_2)\right]/[(\mathbf{q}'-\mathbf{q})^2+m_v^2] \\
&=\left[(g_v+f_v)\bar u(\mathbf{q}',\lambda_1')\gamma_\mu u(\mathbf{q},\lambda_1)-\frac{f_v}{2M}\bar u(\mathbf{q}',\lambda_1')[(q'+q)_\mu+(E'-E)(g_\mu^0-\gamma_\mu\gamma^0)]u(\mathbf{q},\lambda_1)\right] \\
&\quad\times\left[(g_v+f_v)\bar u(-\mathbf{q}',\lambda_2')\gamma^\mu u(-\mathbf{q},\lambda_2)\right. \\
&\qquad\left.-\frac{f_v}{2M}\bar u(-\mathbf{q}',\lambda_2')[(q'+q)_\mu+(E'-E)(g^{\mu0}-\gamma^\mu\gamma^0)]u(-\mathbf{q},\lambda_2)\right]/[(\mathbf{q}'-\mathbf{q})^2+m_v^2]\ ,
\end{aligned} \tag{B7}$$

where λ_i (λ_i'), with $i=1,2$, denotes the helicity of the incoming (outgoing) nucleons, which is defined as the eigenvalue of the operator $\mathbf{s}\cdot\hat{\mathbf{q}}$ with $\mathbf{s}$ the spin operator and $\hat{\mathbf{q}}=\mathbf{q}/|\mathbf{q}|$ the unit momentum operator of the respective nucleon. Working in the two-nucleon c.m. frame, the momenta of the two incoming (outgoing) nucleons are $\mathbf{q}$ and $-\mathbf{q}$ ($\mathbf{q}'$ and $-\mathbf{q}'$). $E=(M^2+\mathbf{q}^2)^{1/2}$ and $E'=(M^2+\mathbf{q}'^2)^{1/2}$. The BbS/Thompson choice [see Appendix A, Eq. (A25)] for the four-momentum transfer is made, i.e., $(q'-q)=(0,\mathbf{q}'-\mathbf{q})$. The Dirac equation is applied repeatedly in the evaluations for the *pv* coupling; the Gordon decomposition[46] is used in the case of the v coupling. [Note that in Eq. (B7), the last line, the term $(q'+q)_\mu$ carries μ as a *subscript* to ensure the correct sign of the space component of that term.] Note that in nuclear matter the tensor coupling constant of the ρ meson, $f_\rho/2M$, should not be changed; i.e., the M in the denominator is not to be replaced by $\tilde M$. Dirac spinors are normalized covariantly:

$$\bar u(\mathbf{q},\lambda)u(\mathbf{q},\lambda)=1\ , \tag{B8}$$

with $\bar u=u^\dagger\gamma^0$. The propagator for vector bosons is

$$i\frac{-g_{\mu\nu}+(q'-q)_\mu(q'-q)_\nu/m_v^2}{-(\mathbf{q}'-\mathbf{q})^2-m_v^2}\ , \tag{B9}$$

where we drop the $(q'-q)_\mu(q'-q)_\nu$ term, which vanishes on-shell, anyhow, since the nucleon current is conserved. The off-shell effect of this term was examined in Ref. 19 and was found to be unimportant.

The relation to the S matrix is

$$\begin{aligned}
\langle p_1'p_2'|S|p_1p_2\rangle&=\delta^{(3)}(\mathbf{q}'-\mathbf{q})\delta^{(3)}(\mathbf{q}'-\mathbf{q}) \\
&\quad-i2\pi\delta^{(4)}(p_1'+p_2'-p_1-p_2) \\
&\quad\times\frac{M^2}{E_q^2}\frac{1}{(2\pi)^3}\mathcal{T}(\mathbf{q}',\mathbf{q})\ ,
\end{aligned} \tag{B10}$$

with p_i ($i=1,2$) the initial and p_i' the final four-momenta of the two interacting nucleons, and with $\mathcal{T}$ as in Eq. (A21) or (A24), the V in those equations being defined as in Eqs. (B5)–(B7).

In practice, it is desirable to have the potential represented in partial waves, since the phase shifts of scattering are only defined in such terms and nuclear

TABLE VI. Parameters of the relativistic OBEP used in this work. The meson parameters given define the potentials. The deuteron and low-energy scattering parameters are predictions by these potentials. The experimental values are given in square brackets. For notation and references to the empirical values, see Ref. 10. It is always used: $f_\rho/g_\rho=6.1$ and $f_\omega/g_\omega=0.0$.

Meson Parameters		Potential A		Potential B		Potential C	
	m_α (MeV)	$g_\alpha^2/4\pi$	Λ_α (GeV)	$g_\alpha^2/4\pi$	Λ_α (GeV)	$g_\alpha^2/4\pi$	Λ_α (GeV)
π	138.03	14.9	1.05	14.6	1.2	14.6	1.3
η	548.8	7	1.5	5	1.5	3	1.5
ρ	769	0.99	1.3	0.95	1.3	0.95	1.3
ω	782.6	20	1.5	20	1.5	20	1.5
δ	983	0.7709	2.0	3.1155	1.5	5.0742	1.5
σ	550	8.3141	2.0	8.0769	2.0	8.0279	1.8
				Deuteron			
$-\epsilon_d$ (MeV)		2.22459		2.22468		2.22450	[2.224575(9)]
P_D (%)		4.47		5.10		5.53	[−]
Q_d (fm^2)		0.274[a]		0.279[a]		0.283[a]	[0.2860(15)]
μ_d (μ_N)		0.8543[a]		0.8507[a]		0.8482[a]	[0.857406(1)]
A_S (fm$^{-1/2}$)		0.8984		0.8968		0.8971	[0.8846(8)]
D/S		0.0255		0.0257		0.0260	[0.0264(12)]
				Low-energy scattering			
a_{np} (fm)		−23.752		−23.747		−23.740	[−23.748(10)]
r_{np} (fm)		2.69		2.67		2.66	[2.75(5)]
a_t (fm)		5.482		5.474		5.475	[5.419(7)]
r_t (fm)		1.829		1.819		1.821	[1.754(8)]

[a]Meson-exchange current contributions not included.

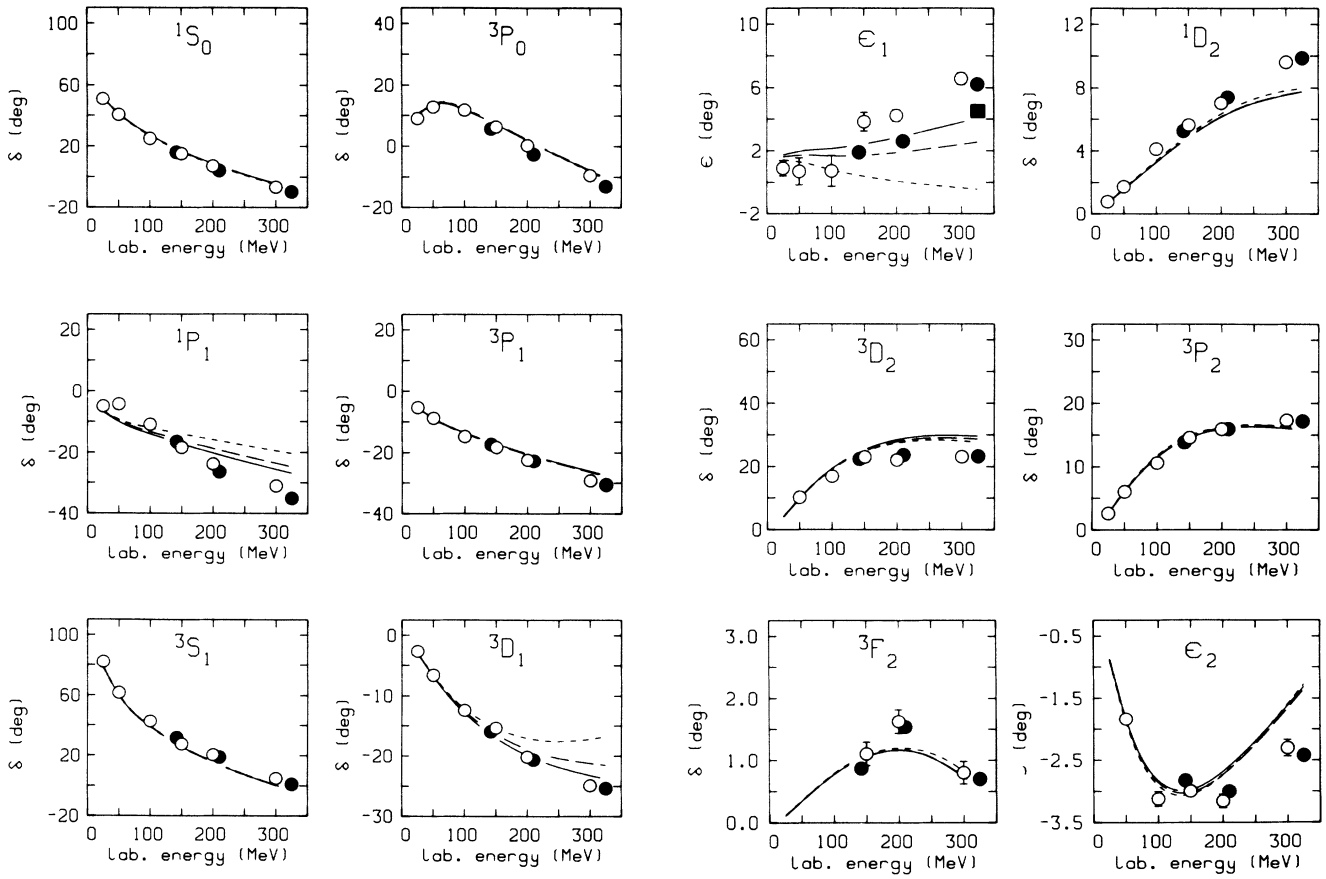

FIG. 5. *NN* phase shifts as described by the three potentials defined in Table VI. Solid line: potential *C*; dashed: *B*; and dotted: *A*. The open circles represent the phase-shift analysis by Arndt *et al.* (Ref. 79), the solid dots and the solid square are from two analyses by Dubois *et al.* (Ref. 80) and Bugg (Ref. 81), respectively.

TABLE VII. Nuclear matter results of a relativistic Dirac-Brueckner calculation applying potential A. Notation as in Table II.

		Relativistic				Nonrel.
k_F (fm^{-1})	$\mathcal{E}/A$ (MeV)	$\tilde{M}/M$	U_S (MeV)	U_V (MeV)	κ (%)	$\mathcal{E}/A$ (MeV)
0.8	−7.27	0.857	−134.3	101.6	22.6	−7.60
0.9	−8.97	0.817	−172.1	131.1	18.1	−9.38
1.0	−10.62	0.777	−209.8	160.6	15.2	−11.01
1.1	−11.96	0.736	−248.5	191.1	11.5	−12.44
1.2	−13.44	0.692	−288.8	222.0	10.6	−14.24
1.3	−14.86	0.647	−331.6	255.0	11.0	−16.35
1.35	−15.32	0.621	−355.7	274.7	11.5	−17.28
1.4	−15.59	0.601	−374.9	289.8	12.1	−18.41
1.5	−14.88	0.557	−416.3	325.7	12.7	−20.25
1.6	−11.96	0.511	−459.6	368.6	14.2	−21.64
1.7	−5.88	0.470	−497.2	412.8	16.9	−22.76
1.8	+4.44	0.435	−530.4	461.6	20.4	−23.38
1.9	19.72	0.409	−554.8	512.0	23.7	−23.54
2.0	41.62	0.390	−572.4	567.5	26.3	−22.60
2.1	71.20	0.371	−590.2	640.3	29.1	−20.42
2.2	106.52	0.366	−595.0	732.5	31.9	−16.74

TABLE VIII. Nuclear matter results of a relativistic Dirac-Brueckner calculation applying potential C. Notation as in Table II.

		Relativistic				Nonrel.
k_F (fm^{-1})	$\mathcal{E}/A$ (MeV)	$\tilde{M}/M$	U_S (MeV)	U_V (MeV)	κ (%)	$\mathcal{E}/A$ (MeV)
0.8	−6.80	0.851	−140.3	108.6	23.0	−7.21
0.9	−8.30	0.812	−176.6	137.2	19.1	−8.79
1.0	−9.69	0.773	−212.9	165.8	16.9	−10.20
1.1	−10.64	0.732	−252.1	197.5	13.6	−11.15
1.2	−11.57	0.688	−292.8	229.8	13.0	−12.46
1.3	−12.25	0.644	−334.0	262.8	13.8	−13.87
1.35	−12.24	0.620	−356.6	281.8	14.5	−14.35
1.4	−11.99	0.601	−374.2	296.4	15.3	−15.02
1.5	−10.06	0.561	−411.8	330.9	16.0	−15.73
1.6	−5.72	0.519	−451.7	373.2	17.5	−15.65
1.7	+1.81	0.482	−486.3	416.6	20.2	−15.01
1.8	13.50	0.450	−516.8	464.6	23.7	−13.50
1.9	29.85	0.426	−538.8	513.8	26.9	−11.22
2.0	52.48	0.409	−554.6	567.7	29.2	−7.39
2.1	82.54	0.391	−571.8	639.4	31.8	−1.75
2.2	119.89	0.379	−583.0	717.7	34.9	+5.88

structure calculations are conventionally performed in an *LSJ* basis. The further formal developments, necessary to arrive at such a partial-wave decomposition for the OBE amplitudes, are presented in all details in Appendix E of Ref. 72 for the *s* and *v* coupling.[77] The final result for the *pv* coupling is given in Appendix A of Ref. 78.

APPENDIX C: RELATIVISTIC MOMENTUM-SPACE OBEP

We give here three examples of relativistic momentum-space OBEP, which are formulated in the framework of the Thompson equation [see Appendix A, Eq. (A24)] and use the *pv* coupling for π and η. The six nonstrange bosons with masses below 1 GeV/c^2 are used. The parameters are given in Table VI. The three potentials differ essentially in the πNN form-factor parameter Λ_π (see below). As a consequence of this, the strength of the tensor force is different, since the nuclear tensor force is essentially provided by the pion. For a detailed (and pedagogical) discussion of the OBE model including the role of the various bosons as well as the choice of the parameters, see Ref. 10.

Phase shifts of low-energy *NN* scattering are shown in Fig. 5. The quantitative nature of these potentials can be seen from this figure and the lower part of Table VI. These potentials are useful for relativistic nuclear structure calculations, which are to be based upon the realistic free-space *NN* interaction. Since in the relativistic approach pair terms (virtual nucleon-antinucleon intermediate states) are taken into account implicitly,[56] the *pv* coupling is necessary; the *ps* coupling leads to unphysically large antiparticle contributions.[40]

Note that a form factor of monopole type

$$\left[\frac{\Lambda_\alpha^2-m_\alpha^2}{\Lambda_\alpha^2+(\mathbf{q}'-\mathbf{q})^2}\right] \tag{C1}$$

is applied to each meson-nucleon vertex. The coupling constants for the two different couplings for *ps* particles are related by

$$g_{ps}=f_{ps}\frac{2M}{m_{ps}}\ . \tag{C2}$$

We use units $\hbar=c=1$ ($\hbar c=197.3286$ MeV fm). In the tables we give the parameters for the ($T=0$ and 1) neutron-proton potentials for which the average nucleon mass $M=938.926$ MeV is used.

In the case of the $^1P_1$ partial wave, there may be some numerical instability in the solution of the integral equation for the $\mathcal{T}$ and G matrices. This is due to the fact that for states with $(S,T)=(0,0)$ (with S and T the total spin and isospin, respectively) the cutoff terms for π and ρ exchange are attractive. Numerical stability in the $^1P_1$ partial-wave contribution can be enforced by setting this unphysical, short-ranged attraction to zero (for short distances or large momenta).

APPENDIX D: MORE NUCLEAR MATTER RESULTS

In Tables VII and VIII we give the relativistic and nonrelativistic nuclear matter results for potentials *A* and *C*.

[1]H. Euler, Z. Phys. **105**, 553 (1937).
[2]K. A. Brueckner, C. A. Levinson, and H. M. Mahmoud, Phys. Rev. **95**, 217 (1954).
[3]H. A. Bethe, Phys. Rev. **103**, 1353 (1956).
[4]J. Goldstone, Proc. R. Soc. (London) A **239**, 267 (1957).
[5]R. Jastrow, Phys. Rev. **98**, 1479 (1955).
[6]B. D. Day, Rev. Mod. Phys. **39**, 719 (1967).
[7]M. I. Haftel and F. Tabakin, Nucl. Phys. **A158**, 1 (1970).
[8]H. A. Bethe, Annu. Rev. Nucl. Sci. **21**, 93 (1971).
[9]D. W. L. Sprung, Adv. Nucl. Phys. **5**, 225 (1972).
[10]R. Machleidt, Adv. Nucl. Phys. **19**, 189 (1989).
[11]T. Hamada and I. D. Johnston, Nucl. Phys. **34**, 382 (1962).
[12]B. D. Day, Phys. Rev. Lett. **47**, 226 (1981).
[13]H. A. Bethe and M. B. Johnson, Nucl. Phys. **A230**, 1 (1974).
[14]R. V. Reid, Ann. Phys. (N.Y.) **50**, 411 (1968).
[15]R. Machleidt, Ph.D. thesis, University of Bonn, 1973 (unpublished).
[16]R. B. Wiringa, R. A. Smith, and T. L. Ainsworth, Phys. Rev. C **29**, 1207 (1984).
[17]B. D. Day and R. B. Wiringa, Phys. Rev. C **32**, 1057 (1985).
[18]M. Lacombe *et al.*, Phys. Rev. C **21**, 861 (1980).
[19]K. Holinde and R. Machleidt, Nucl. Phys. **A247**, 495 (1975).
[20]G. Schierholz, Nucl. Phys. **B40**, 335 (1972).
[21]T. Ueda, M. Nack, and A. E. S. Green, Phys. Rev. C **8**, 2061 (1973).
[22]F. Coester, S. Cohen, B. D. Day, and C. M. Vincent, Phys. Rev. C **1**, 769 (1970).
[23]B. D. Day, Phys. Rev. C **24**, 1203 (1981).
[24]B. D. Day, Comments Nucl. Part. Phys. **11**, 115 (1983).
[25]For reviews, see, e.g., B. D. Day, Rev. Mod. Phys. **50**, 495 (1978) and A. D. Jackson, Annu. Rev. Nucl. Part. Sci. **33**, 105 (1983), and references therein.
[26]O. Benhar, C. Ciofi degli Atti, S. Fantoni, and S. Rosati, Nucl. Phys. **A238**, 127 (1979); V. R. Pandharipande and R. B. Wiringa, Rev. Mod. Phys. **51**, 821 (1979), and references therein.
[27]B. Friedman and V. R. Pandharipande, Nucl. Phys. **A361**, 502 (1981).
[28]G. A. Crawford and G. A. Miller, Phys. Rev. C **36**, 2569 (1987).
[29]T. Goldman, K. R. Maltman, G. J. Stephenson, and K. E. Schmidt, Nucl. Phys. **A481**, 621 (1988).
[30]L. D. Miller and A. E. S. Green, Phys. Rev. C **5**, 241 (1972).
[31]R. Brockmann, Phys. Rev. C **18**, 1510 (1978); R. Brockmann and W. Weise, Nucl. Phys. **A355**, 365 (1981).
[32]C. J. Horowitz and B. D. Serot, Nucl. Phys. **A368**, 503 (1981).
[33]B. D. Serot and J. D. Walecka, Adv. Nucl. Phys. **16**, 1 (1986).
[34]L. G. Arnold, B. C. Clark, and R. L. Mercer, Phys. Rev. C **19**, 917 (1979).
[35]S. J. Wallace, Annu. Rev. Nucl. Part. Sci. **37**, 267 (1987).
[36]J. D. Walecka, Ann. Phys. (N.Y.) **83**, 491 (1974).
[37]M. R. Ansatasio, L. S. Celenza, W. S. Pong, and C. M. Shakin, Phys. Rep. **100**, 327 (1983).
[38]L. S. Celenza and C. M. Shakin, *Relativistic Nuclear Physics: Theories of Structure and Scattering,* Vol. 2 of *Lecture Notes in Physics* (World Scientific, Singapore, 1986).
[39]R. Brockmann and R. Machleidt, Phys. Lett. **149B**, 283 (1984).
[40]R. Machleidt and R. Brockmann, in *Proceedings of the Los Alamos Workshop on Dirac Approaches in Nuclear Physics,* edited by J. R. Shepard, C. Y. Cheung, and R. L. Boudrie (Publisher, Los Alamos, NM, 1985), p. 328.
[41]B. ter Haar and R. Malfliet, Phys. Rep. **149**, 207 (1987).
[42]C. J. Horowitz and B. D. Serot, Phys. Lett. **137B**, 287 (1984).
[43]C. J. Horowitz and B. D. Serot, Nucl. Phys. **A464**, 613 (1987).
[44]R. Machleidt and R. Brockmann, Phys. Lett. **160B**, 364 (1985).
[45]H. Müther, R. Machleidt, and R. Brockmann, Phys. Rev. C **42**, 1981 (1990), the following paper.
[46]J. D. Bjorken and S. D. Drell, *Relativistic Quantum Mechanics* (McGraw-Hill, New York, 1964).
[47]R. H. Thompson, Phys. Rev. D **1**, 110 (1970).
[48]E. E. Salpeter and H. A. Bethe, Phys. Rev. **84**, 1232 (1951).
[49]R. Blankenbecler and R. Sugar, Phys. Rev. **142**, 1051 (1966).
[50]See Fig. 10.7 of Ref. 10.
[51]K. Erkelenz, Phys. Rep. C **13**, 191 (1974).
[52]See dot-dashed curve in Fig. 16 of Ref. 43.
[53]A. B. Migdal, *Theory of Finite Fermi Systems and Applications to Atomic Nuclei* (Wiley, New York, 1967).
[54]B. Keister and R. B. Wiringa, Phys. Lett. B **173**, 5 (1986).
[55]M. Jaminon and C. Mahaux, Phys. Rev. C **40**, 354 (1989).
[56]G. E. Brown *et al.*, Comments Nucl. Part. Phys. **17**, 39 (1987).
[57]J. P. Blaizot, Phys. Rep. **65**, 171 (1980).
[58]S. Krewald, K. Nakayama, and J. Speth, Phys. Rep. **161**, 103 (1988).
[59]J. W. Harris *et al.*, Phys. Rev. Lett. **58**, 463 (1987).
[60]K. H. Kampert *et al.*, Mod. Phys. Lett. A **3**, 849 (1988).
[61]E. Baron, J. Cooperstein, and S. Kahana, Phys. Rev. Lett. **55**, 126 (1985).
[62]P. Grangé and A. Lejeune, Nucl. Phys. **A327**, 335 (1979); C. Mahaux, *ibid.* **A328**, 24 (1979).
[63]M. F. Jiang, R. Machleidt, and T. T. S. Kuo (unpublished).
[64]J. Fleischer and J. A. Tjon, Phys. Rev. D **21**, 87 (1980).
[65]M. J. Zuilhof and J. A. Tjon, Phys. Rev. C **24**, 736 (1981).
[66]J. Fleischer and J. A. Tjon, Nucl. Phys. **B84**, 375 (1975).
[67]F. Gross, Phys. Rev. C **26**, 2203 (1982).
[68]R. J. Yaes, Phys. Rev. D **3**, 3086 (1971).
[69]M. H. Partovi and E. L. Lomon, Phys. Rev. D **2**, 1999 (1970).
[70]B. ter Haar (private communication).
[71]R. Machleidt (unpublished).
[72]R. Machleidt, K. Holinde, and C. Elster, Phys. Rep. **149**, 1 (1987).
[73]N. Nakanishi, Prog. Theor. Phys. (Kyoto) Suppl. **43**, 1 (1969).
[74]R. Woloshyn and A. D. Jackson, Nucl. Phys. **B64**, 269 (1973).
[75]G. E. Brown and A. D. Jackson, *The Nucleon-Nucleon Interaction* (North-Holland, Amsterdam, 1976).
[76]Strictly speaking, we give here the potential which is defined as i times the Feynman amplitude; furthermore, there is a factor of i in each vertex and meson propagator; as $i^4=1$, we can ignore these four factors of i.
[77]Note that there is an error in Eq. (E52.b) of Ref. 72 where it should read

$$^{34}V_{tt}^{J}=C_{tt}[-(q'^2+q^2+4E'E)q'qI_J^{(0)}(m_v)-\cdots]\ .$$

[78]R. Machleidt, in *Relativistic Dynamics and Quark-Nuclear Structure,* edited by M. B. Johnson and A. Picklesimer (Wiley, New York, 1986), p. 71.
[79]R. A. Arndt, L. D. Roper, R. A. Bryan, R. B. Clark, B. J. VerWest, and P. Signell, Phys. Rev. D **28**, 97 (1983).
[80]R. Dubois *et al.*, Nucl. Phys. **A377**, 554 (1982).
[81]D. V. Bugg (private communication).